

This work was written as part of one of the author's official duties as an Employee of the United States Government and is therefore a work of the United States Government. In accordance with 17 U.S.C. 105, no copyright protection is available for such works under U.S. Law.

Public Domain Mark 1.0

<https://creativecommons.org/publicdomain/mark/1.0/>

Access to this work was provided by the University of Maryland, Baltimore County (UMBC) ScholarWorks@UMBC digital repository on the Maryland Shared Open Access (MD-SOAR) platform.

**Please provide feedback**

Please support the ScholarWorks@UMBC repository by emailing [scholarworks-group@umbc.edu](mailto:scholarworks-group@umbc.edu) and telling us what having access to this work means to you and why it's important to you. Thank you.

# FORECASTING CORN YIELD WITH IMAGING SPECTROSCOPY

Lawrence A. Corp<sup>1</sup>, Elizabeth M. Middleton<sup>2</sup>, Craig S.T. Daughtry<sup>3</sup>, Andrew L. Russ<sup>3</sup>,  
Petya K.E. Campbell<sup>4</sup>, K. Fred Huemrich<sup>4</sup>, Yen-Ben Cheng<sup>5</sup>

<sup>1</sup>Sigma Space Corporation, Lanham, MD 20706

<sup>2</sup>Biospheric Sciences Branch, NASA/GSFC, Greenbelt, MD 20771

<sup>3</sup>Hydrology & Remote Sensing Laboratory, USDA ARS, Beltsville, MD, 20705

<sup>4</sup>Joint Center for Earth Systems Technology, UMBC, Baltimore, MD 21250

<sup>5</sup>Earth Resources Technology Inc., Annapolis Junction, MD 20701

## ABSTRACT

Corn is the most widely produced grain in the United States with 87 million acres planted in 2009 accounting for more than 90 percent of total value and production of feed grains. Half of United States' corn production is used in livestock feed with the remainder processed into a multitude of food and industrial products including starch, sweeteners, corn oil, beverage and industrial alcohol, and fuel ethanol. With increased focus on renewable energy, an unusual link between corn and oil commodities has been created increasing the demand for the grain in ethanol production. As a result, monitoring crop performance is vital for yield forecasting and developing timely remediation strategies to optimize crop performance. Several factors including water availability, nitrogen (N) supply, soil organic matter, disease, and supply of other nutrients, have a significant impact on crop growth and grain yields. Imaging spectroscopy can provide timely, spatially explicit information for managing agricultural ecosystems. The HypsIRI mission called for by the NRC Decadal Survey [11] identifies the need for a near term space-borne hyperspectral imaging spectrometer to globally map early signs of ecosystem change through altered physiology. The primary instrument on the proposed NASA HypsIRI mission is a hyperspectral (10 nm FWHM) mapper with a 60 m ground resolution and a 19 day global revisit, which will enable imaging spectroscopy with high temporal repeat to capture the impact of environmental perturbations on ecosystem productivity. Recent advances in airborne hyperspectral imaging systems [i.e., AVIRIS [7], AISA EAGLE & Hawk (Specim, Oulu, Finland)] along with Earth Observing One (EO-1) Hyperion satellite data have made it possible to obtain high resolution spatial and full range visible (VIS) to short wave infrared (SWIR) spectral information that can be further employed to explore vegetation productivity and change in both agricultural and surrounding ecosystems to further define algorithms and products applicable to the HypsIRI mission. From hyperspectral data, numerous statistical and spectroscopic approaches have been developed that use features in

vegetation spectral curves to gain insight to biophysical parameters, including: biomass, pigments, tissue water content, and the amount of lignin, cellulose, and foliar N [1, 3, 5, 6, 9, 10, 12, 13, 14]. In the case of optically dense vegetation, the spectral derivative has been shown to be indicative of the abundance and activity of the absorbers in the leaves [2, 4]. Further, linear unmixing and spectral angle matching techniques take advantage of the high dimensionality of hyperspectral data and can be used alone or in conjunction with other vegetation indices for ecosystem assessment [8]. Here we will further investigate these spectroscopic techniques to enhance corn yield forecasting capabilities.

## 1. EXPERIMENT SITE

The experiment site located at USDA Beltsville Agricultural Research Center is part of an intensive multi-disciplinary project, Optimizing Production Inputs for Economic and Environmental Enhancement (OPE3). Ground sampling occurred in 2009 across the OPE3 field site that had been planted with field corn (*Zea mays* L. 'Pioneer 33A14'). 12 N treatment plots were established within the OPE field site each measuring 18.2 m wide (containing 24 rows) by 28.3 m long. The experimental design was a randomized complete block with treatment groups of 280, 140, 70, and 0 kg N/ha, which provided a range of plant growth and conditions equivalent to 150%, 100%, 50% and 0% of additional soil N. *In situ* georeferenced canopy measurements were made during reproductive stages R1 to R3: leaf area index (LAI), fraction of absorbed photosynthetically active radiation (fAPAR), grain yield (kg/ha), and canopy R. LAI was measured with the LI-2000 Plant Canopy Analyzer (LI-Cor Inc., Lincoln NE, USA) using a single above canopy and four below canopy data points at each *in situ* measurement location. Grain yields were obtained with a yield monitor (AgLeader 2000, Roswell, GA) measuring the grain flow from the combine at harvest interfaced with a differential GPS.

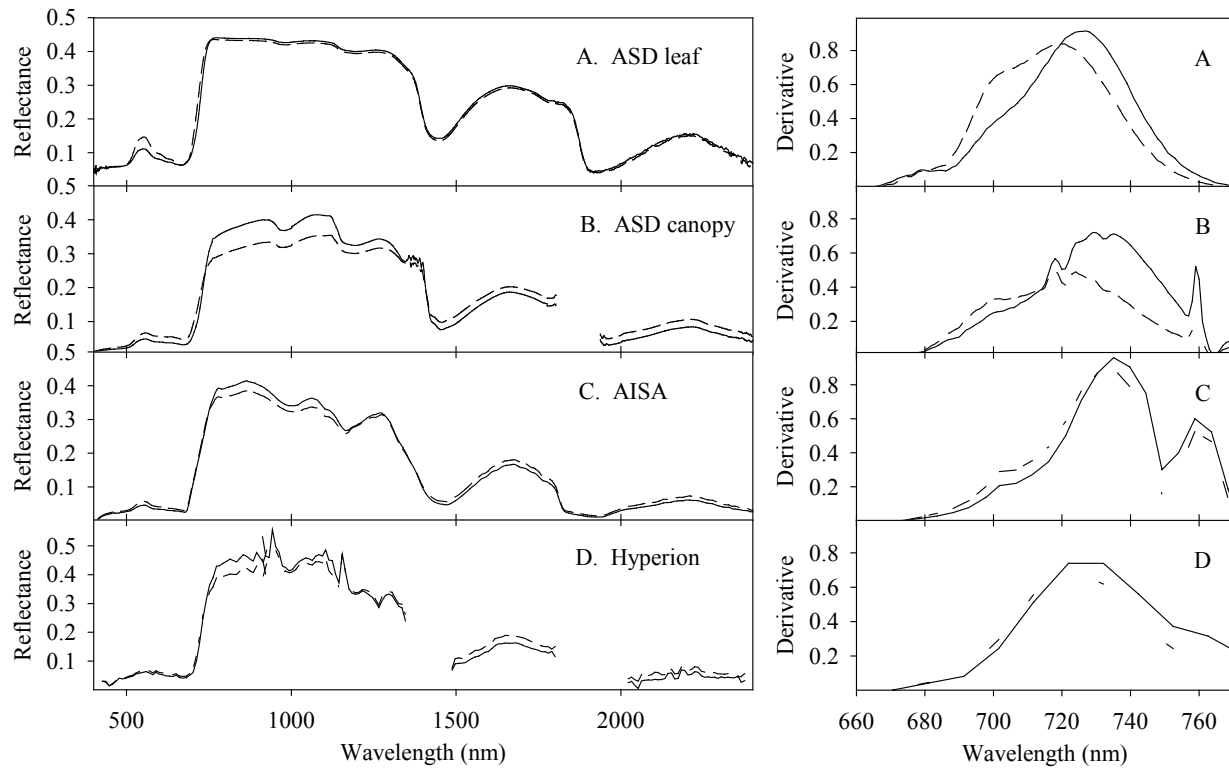


Figure 1. Reflectance and reflectance derivative spectra (x100) for high N (solid) and low N (dashed) field corn at four observation levels; A) leaf integrating sphere with ASD spectral radiometer, B) above canopy at 1m with ASD spectral radiometer, C) AISA aircraft hyperspectral sensor, D) EO-1 Hyperion orbital hyperspectral imager.

## 2. MULTI-SCALE SPECTRAL OBSERVATIONS

A spectral radiometer (ASD-FR FieldSpec Pro, Analytical Spectral Devices, Inc., Boulder CO, USA) was used to measure leaf and canopy radiance from 350 – 2500 nm at nadir. Aircraft multispectral R imagery was acquired over the site with the Airborne Imaging Spectrometer for Applications (AISA Eagle & Hawk, flown by SpecTIR, Easton MD, USA). The AISA imaging spectrometer was configured with 360 bands ranging from 396 nm to 2460 nm with a sampling resolution of 5 nm. The instrument was flown at 400 m with a 2 m per pixel ground resolution. Hyperspectral satellite data over the study site was acquired at a 30 m ground resolution with EO-1 Hyperion sensor from a 705 km sun synchronous orbit with a 10 AM overpass. The Hyperion Level 1R data product has 220 contiguous radiometrically corrected spectral bands with a 10 nm FWHM covering the spectral range from 400-2500 nm.

Spectral observations acquired at these four measurement levels ranging from leaf to satellite are shown in Figure 1. Full range spectral reflectance (R) for each measurement scale are shown for the mean of 10 randomly selected points from the populations representing high

yielding area of the field (solid lines) and low yielding regions of the field (dashed lines). A generalized response of reduced crop performance on spectral R is apparent across measurement scales and manifests itself as: (i) increased response in the region from 500 – 600 nm; (ii) a shift in the red-edge R toward the blue; (iii) a more pronounced double peak in the red-edge derivative spectra; (iv) decreased NIR R from 775 – 1300 nm; and (v) increased SWIR R from 1500 – 2400 nm.

From the leaf level spectra plotted in Figure 1a, it is clear the ASD FR-PRO spectral radiometer coupled to an integrating sphere produced smooth aberration free spectra over the full range of the spectrometer. Leaf level observations from low performing area of the field exhibited a 5% increase in the green R peak near 550 nm along with a more pronounced red-edge derivative feature at 705 nm. The wavelength maximum of the major derivative feature occurs near 730 nm for corn in high performing regions, which was shifted toward the blue as crop stress increased. In canopy level spectra, the red-edge derivative features although still apparent becomes more obscured by the atmospheric O<sub>2</sub> band at 760 nm and the water vapor bands near 720 nm, while the impact of varying canopy structure leads to pronounced changes in NIR R from 775 – 1300 nm.

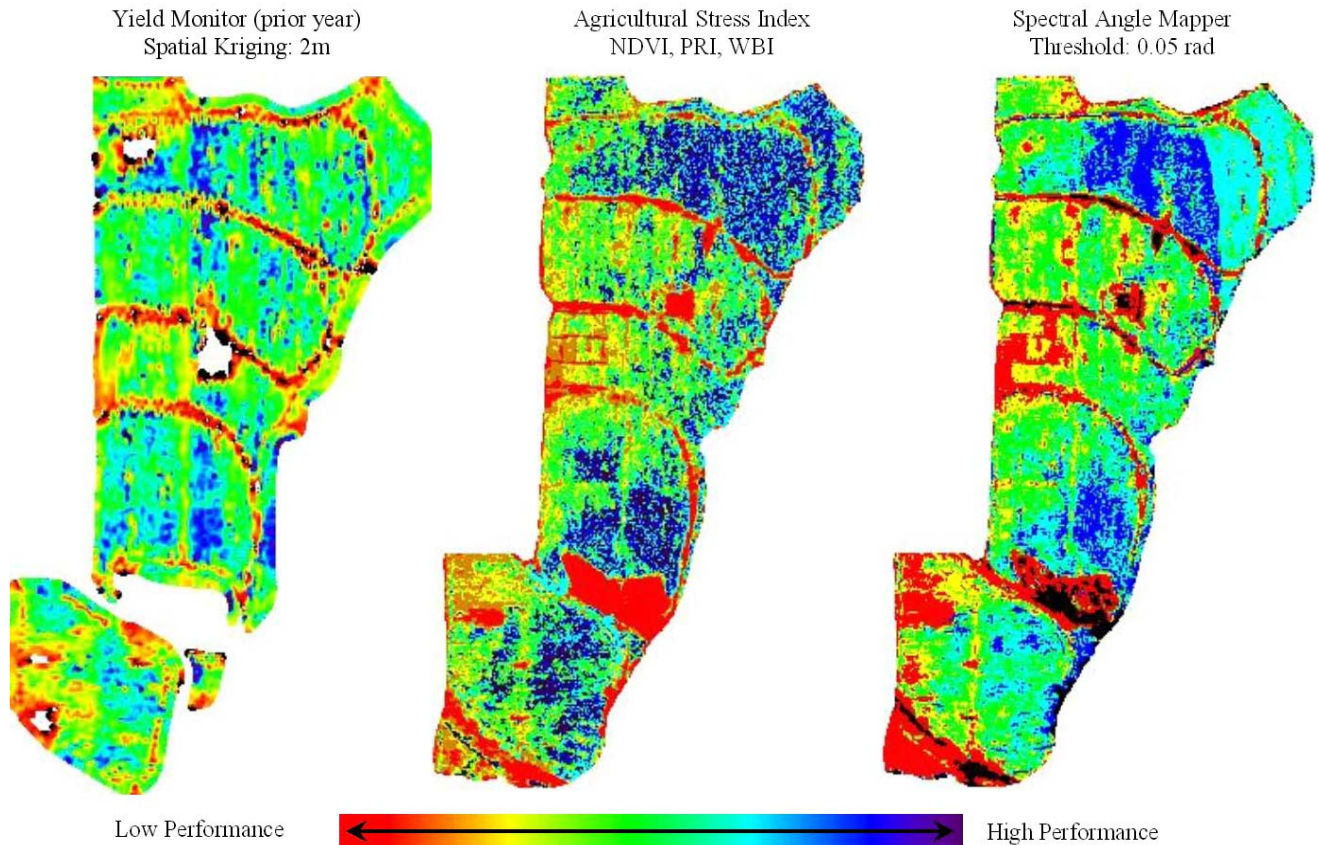


Figure 2. Classification of field corn performance derived from AISA aircraft imagery with VIS to SWIR 360 band spectral coverage compared against a prior year yield monitor data.

### 3. IMAGING SPECTROSCOPY TO ESTIMATE CROP PRODUCTION

Spectral R features are well conserved between the ASD canopy and AISA aircraft observation levels. The AISA Eagle and Hawk sensor as they were configured for this acquisition offered 20 spectral bands defining the red-edge spectral region. At this spectral sampling interval the double red-edge derivative feature was evident. The derivative feature at 705 nm is reduced and barely discernable at the 10 nm sampling resolution of Hyperion while Dmax and the red-edge shift are still prominent (Fig. 1d). The EO-1 Hyperion spectra are strongly impacted by atmospheric absorption from water vapor and CO<sub>2</sub> with R data in the spectral region from 1.3 – 1.5  $\mu\text{m}$  and 1.8 – 2.0  $\mu\text{m}$  being not suitable for the spectral remote sensing of vegetation parameters. Despite the impact of increased atmospheric scatter in the visible and strong absorption by atmospheric constituents in the NIR to SWIR regions, many of the spectral characteristics attributed to reduced productivity are still evident in the satellite observations, demonstrating the utility of 10 nm sampling resolution for monitoring ecosystem health from space.

Grain yields over the OPE study site varied from 7.23 Mg/ha (red-yellow) to 3.78 Mg/ha (blue-green) with high and low performing areas being attributed to variable management practices, soil properties, and hydrological processes (Fig 2, left). The ENVI Agricultural Stress Classification Tool (ITT Visual Information Solutions, Boulder CO, USA) was used to create a spatial map showing the distribution of crop stress. A mask was generated to separate OPE field corn from the surrounding riparian forest and neighboring fields. Next, the classification scheme was applied based on two normalized difference vegetation indices (i.e., an index for the R difference divided by the R sum for two designated bands), namely; the original Normalized Difference Vegetation Index (NDVI: using red and NIR bands at 680 nm and 800 nm) which is affected by pigment levels and LAI, the photochemical reflectance index (PRI, using bands centered at 531 nm and 570 nm) which is sensitive to light use efficiency, and the water band index (WBI: using a ratio of bands at 900 nm and 970 nm) sensitive to canopy water content (Fig 2, center). The Spectral Angle Mapper (SAM)

is a physically-based spectral classification that uses the high fidelity of hyperspectral data to determine the spectral similarity between image pixels. AISA endmember spectra were selected based on field observations and prior spatial knowledge of crop performance over the field site. SAM was used to compare spectra by calculating the angle between spectra and treating them as vectors in a 360 dimensional space equal to the number of spectral bands. Smaller angles represent closer matches to the reference spectrum while pixels further away than the specified maximum angle threshold of 0.05 radians were not classified (Fig 2, right). Spatial associations are evident between these two spectroscopic classifications and yield data with associations visually apparent. The soil berms delineating the four hydrologically bounded watersheds are visible in the imagery with low index and yield values. Natural variation is evident with spatial associations between yield monitor and R indices apparent in several clusters of low and high performing areas of the field. These observations imply these early to mid-day R indices remotely observed from a corn canopy in the early reproductive growth phases express a significant relationship to grain yields obtained at harvest.

#### 4. CONCLUSIONS

Since crops have different planting dates, phenological cycles, LAI, and other biophysical properties, the vegetation indices and spectral signals within and between crop types may not lead to a quantitative solution for tracking productivity. However, the remotely sensed observations of high temporal frequency combination with prior years yield performance could offer substantial quantitative improvements in yield forecasting. The results from this study indicate that the SAM technique with careful selection of spectral endmembers can be used alone or in conjunction with other vegetation indices to improve yield estimation using hyperspectral imagery.

#### 5. REFERENCES

- [1] Corp, L.A., Middleton, E.M., Campbell, P.K.E., Huemmrich, K.F., Cheng, Y.B., Daughtry, C.S.T., "Remote Sensing techniques to monitor Nitrogen driven Carbon dynamics in vegetation," *SPIE Optics Photonics, Optical Engineering plus Applications, Remote Sensing and Modeling of Ecosystems for Sustainability*, 2009.
- [2] Curran, P. J., "Remote-Sensing Of Foliar Chemistry," *Remote Sensing Of Environment*, 30, 271-278, 1989.
- [3] Daughtry, C.S.T., E.R. Hunt Jr., and J.E. McMurtrey III., "Assessing Crop Residue Cover Using Shortwave Infrared Reflectance," *Remote Sensing of Environment*, 90:126-134, 2004.
- [4] Filella, I., & Pen˜uelas, J., "The red edge position and shape as indicators of plant chlorophyll content, biomass and hydric status," *International Journal of Remote Sensing*, 15(7), 1459–1470, 1994.
- [5] Gamon, J.A., L. Serrano, and J.S. Surfus, "The Photochemical Reflectance Index: An Optical Indicator of Photosynthetic Radiation Use Efficiency Across Species, Functional Types and Nutrient Levels," *Oecologia*, 112:492-501, 1997.
- [6] Goetz, A. F. H., & Curtiss, B., "Hyperspectral imaging of the Earth: Remote analytical chemistry in an uncontrolled environment," *Field Analytical Chemistry and Technology*, 1, 67-76, 1996.
- [7] Green, R.O., Eastwood, M.L., Sarture, C.M., Chrien, T.G., Aronsson, M., Chippendale, B.J., Faust, J.A., Pavri, B.E., Chovit, C.J., Solis, M., Olah, M.R., Williams, O., "Imaging Spectroscopy and the Airborne Visible/Infrared Imaging Spectrometer (AVIRIS)", *Remote Sensing of Environment*, 65(3) 227-248, 1998.
- [8] Kruse, F. A., A. B. Lefkoff, J. B. Boardman, K. B. Heidebrecht, A. T. Shapiro, P. J. Barloon, and A. F. H. Goetz, "The Spectral Image Processing System (SIPS) - Interactive Visualization and Analysis of Imaging spectrometer Data." *Remote Sensing of the Environment*, v. 44, p. 145 – 163, 1993.
- [9] Middleton, E.M., Y.-B. Cheng, T. Hilker, T.A. Black, P. Krishnan, N.C. Coops, and K.F. Huemmrich, "Linking Foliage Spectral Responses to Canopy Level Ecosystem Photosynthetic Light Use Efficiency at a Douglas-fir Forest in Canada," *Canadian J. Rem. Sen.*, 35:2, 166-188, 2009.
- [10] Pen˜uelas, J., I. Filella, C. Biel, L. Serrano, and R. Save, "The Reflectance at the 950-970 Region as an Indicator of Plant Water Status," *International Journal of Remote Sensing*, 14:1887-1905, 1995.
- [11] Space Studies Board of the National Research Council, *Earth Science and Applications from Space: National Imperatives for the Next Decade and Beyond*, (pp. 113-115). Washington D.C., The National Academies Press, 2007.
- [12] Tucker, C.J., "Red and Photographic Infrared Linear Combinations for Monitoring Vegetation," *Remote Sensing of the Environment*, 8:127-150, 1979.
- [13] Yang C., Everitt, J.H., Bradford, J.M., "Yield Estimation from Hyperspectral Imagery Using Spectral Angle Mapper (SAM)", *American Society of Agricultural and Biological Engineers*, 51(2): 729-737, 2008.
- [14] Zhao, D. H., "Hyperspectral characteristic analysis of a developing cotton canopy under different nitrogen treatments," *Agronomie*, 24, 463-471, 2004.